



OPEN ACCESS

EDITED BY

Marcello Natalicchio,
University of Turin, Italy

REVIEWED BY

Shifeng Dai,
China University of Mining and Technology,
Beijing, China
James Hower,
University of Kentucky, United States

*CORRESPONDENCE

Haley H. Coe,
✉ haley.coe@utah.edu

RECEIVED 02 February 2024

ACCEPTED 10 April 2024

PUBLISHED 26 April 2024

CITATION

Coe HH, Birgenheier LP, Fernandez DP,
Gall RD, Vanden Berg MD and Giebel A (2024),
Rare earth element enrichment in coal and
coal-adjacent strata of the Uinta Region, Utah
and Colorado.
Front. Earth Sci. 12:1381152.
doi: 10.3389/feart.2024.1381152

COPYRIGHT

© 2024 Coe, Birgenheier, Fernandez, Gall,
Vanden Berg and Giebel. This is an
open-access article distributed under the
terms of the [Creative Commons Attribution
License \(CC BY\)](https://creativecommons.org/licenses/by/4.0/). The use, distribution or
reproduction in other forums is permitted,
provided the original author(s) and the
copyright owner(s) are credited and that the
original publication in this journal is cited, in
accordance with accepted academic practice.
No use, distribution or reproduction is
permitted which does not comply with
these terms.

Rare earth element enrichment in coal and coal-adjacent strata of the Uinta Region, Utah and Colorado

Haley H. Coe^{1*}, Lauren P. Birgenheier¹, Diego P. Fernandez¹,
Ryan D. Gall², Michael D. Vanden Berg² and Andrew Giebel³

¹Geology and Geophysics Department, University of Utah, Salt Lake City, UT, United States, ²Utah Geological Survey, Salt Lake City, UT, United States, ³Colorado Geological Survey, Golden, CO, United States

This study aims to quantify rare earth element enrichment within coal and coal-adjacent strata in the Uinta Region of central Utah and western Colorado. Rare earth elements are a subset of critical minerals as defined by the U.S. Geological Survey. These elements are used for a wide variety of applications, including renewable energy technology in the transition toward carbon-neutral energy. While rare earth element enrichment has been associated with Appalachian coals, there has been a more limited evaluation of western U.S. coals. Here, samples from six active mines, four idle/historical mines, four mine waste piles, and seven stratigraphically complete cores within the Uinta Region were geochemically evaluated using portable X-ray fluorescence ($n = 3,113$) and inductively coupled plasma-mass spectrometry ($n = 145$) elemental analytical methods. Results suggest that 24%–45% of stratigraphically coal-adjacent carbonaceous shale and siltstone units show rare earth element enrichment (>200 ppm), as do 100% of sampled igneous material. A small subset (5%–8%) of coal samples display rare earth element enrichment, specifically in cases containing volcanic ash. This study proposes two multi-step depositional and diagenetic models to explain the enrichment process, requiring the emplacement and mobilization of rare earth element source material due to hydrothermal and other external influences. Historical geochemical evaluations of Uinta Region coal and coal-adjacent data are sparse, emphasizing the statistical significance of this research. These results support the utilization of active mines and coal processing waste piles for the future of domestic rare earth element extraction, offering economic and environmental solutions to pressing global demands.

KEYWORDS

rare earth elements, critical minerals, coal, Uinta Region, energy transition, Cretaceous, Blackhawk Formation, Mesaverde group

1 Introduction

The contemporary world is transitioning away from a dependence on traditional fossil fuels and toward a future of carbon-neutral energy. Rare earth elements (REEs) include the 15 elements within the lanthanide series as well as scandium (Sc) and

yttrium (Y) (IUPAC, 2005; Humphries, 2011; Zhou et al., 2016). These elements are valuable as they are used in everyday technology (television/computer/phone screens), medical devices, auto- and fluid catalysts, metallurgy, military defense systems, clean energy, and more (Leslie et al., 2010; Humphries, 2011; Long et al., 2012; Weng et al., 2014; Hower et al., 2016; Zhou et al., 2016). Carbon-neutral energy technology, including wind power turbines, solar power, electric vehicles, rechargeable batteries, and energy-efficient lighting, also require these specific elements (Leslie et al., 2010; Humphries, 2011; Alonso et al., 2012; Long et al., 2012; Seredin et al., 2013; Weng et al., 2014; Zhou et al., 2016; Zhou et al., 2017). With the growth of these technologies emerges a global demand for REEs and economic pressure on the current supply chain (Leslie et al., 2010; Humphries, 2011; Alonso et al., 2012; Long et al., 2012; Zhou et al., 2016; Zhou et al., 2017).

China dominates the REE industry, supplying over 90% of the global demand (Krahulec and Bon, 2010; Cordier, 2012; Weng et al., 2014; Zhou et al., 2017; Mancheri et al., 2019; Dushyantha et al., 2020). Within the past 20 years, China has increased export taxes and limited the export of REEs, prompting the exploration of REE extraction elsewhere in the world (Krahulec and Bon, 2010; Weng et al., 2014; Zhang et al., 2015; Zhou et al., 2016). The United States has great potential for REE and critical mineral extraction as coal deposits offer alternative sources for REEs and the U.S. contains the largest coal resource base around the globe (Seredin et al., 2013; Dai et al., 2016; Hower et al., 2016; Lin et al., 2018).

Economically viable REEs are typically associated with igneous rock (Long et al., 2012; Weng et al., 2014). However, previous studies have documented REE enrichment within coals and coal by-products (Seredin and Dai, 2012; Zhou et al., 2016). REE-enrichment within coals has been demonstrated across regions of the U.S., including but not limited to North Dakota (Laudal et al., 2018), Indiana (Chatterjee et al., 2022), the Powder River Basin of Wyoming (Bagdonas et al., 2022), and the Eocene Jackson Group of Texas (Hower et al., 2023a). Lin et al. (2018) evaluated REE enrichment across multi-region U.S. coals utilizing the USGS COALQUAL Database 3.0. These data, comprising 7,657 non-weathered, full-bed coal samples, contain a mean concentration of 65.5 ppm total REEs on a moisture-free whole coal basis. These values, however, reflect an over-sampling bias within the Appalachian Region ($n = 4,214$). As only $n = 89$ coal samples from the Uinta Region have been evaluated in this context, further analysis is required. However, despite the small sample size, approximately 1%–15% of Uinta coals are considered promising and highly promising for REE enrichment (Lin et al., 2018).

This research intends to analyze the coal seams and adjacent stratigraphic units from various active mine locations to understand REE enrichment in Utah and Colorado coal fields. Research goals included 1) determining the geologic trends in REE enrichment in the Uinta Region (*sensu East, 2013*) coal and coal-associated strata, specifically the stratigraphic and geographic patterns, and 2) developing hypotheses regarding geologic controls on REE enrichment based on observed spatial trends.

This study significantly enhances historically sparse REE coal datasets from the Uinta Region and includes a more comprehensive evaluation of coals and coal-adjacent strata within a geologic context. While focusing exclusively on the Uinta Region, the quantity of data reported in this study is significantly larger than

other regional datasets available to date, comprising 3,113 pXRF datapoints and 145 ICP-MS datapoints. This dataset rivals the volume of data from the Appalachian Region collated by Lin et al. (2018) from the USGS COALQUAL Database 3.0 ($n = 4,214$). The newly reported data in this study have the added benefit of geologic, lithologic, and stratigraphic context that is missing from the comparably sized Appalachian Region database. With an order of magnitude more data than previously available from the Uinta Region, coupled with valuable geologic context, this study presents a globally unique dataset. The emerging geologic trends observed in the regional data merit further application in other regions worldwide.

As coal is already utilized in the western U.S. as an energy source, existing coal mines have the potential for possible co-extraction of REEs. Theoretically, U.S. coals contain enough critical elements to meet national demands for years following commercial extraction (Lin et al., 2018). Therefore, the extraction of REEs from within the United States would provide an economic benefit as well as an environmental value.

2 Materials and methods

2.1 Geologic setting

Coal-bearing strata in the Uinta Region include the Cretaceous Naturita (formerly known as the Dakota) Sandstone, Ferron Sandstone, and Blackhawk Formation of Utah as well as the Cretaceous Mesaverde Group of western Colorado (Figure 1). This study focuses largely on the Blackhawk Formation of Utah and the Mesaverde Group of western Colorado. The bulk of the data for this study comes from these two geologic units, with a very minor amount of data from the Ferron Sandstone.

During the Cretaceous period, the Uinta Region was a flexural, subsiding foreland basin developed as a result of crustal thickening and loading of clastic sediment from the Sevier fold-and-thrust belt to the west, deposited in coastal plain settings around the shoreline of the Western Interior Seaway (Kauffman and Caldwell, 1993; Roberts and Kirschbaum, 1995; Liu et al., 2014).

The Blackhawk Formation is a thick, mid-Campanian deposit within the basin recording the fluvial, coastal plain, and shallow marine deposition prograding into the seaway, represented by the Mancos Shale (Taylor et al., 2004). Along with the overlying Castlegate Sandstone and underlying Star Point Sandstone, these lithostratigraphic units record the eastward progradation of Sevier-sourced siliciclastic material into the offshore deposits of the Mancos Shale (Young, 1955; Yoshida, 2000; Hampson, 2010).

The Blackhawk Formation provides the primary target for underground mining operations within the Wasatch Plateau and Book Cliffs, as the unit contains abundantly thick, laterally extensive, continuous coal beds (Roberts and Kirschbaum, 1995; Dubiel, 2000). Along with bituminous coal, the formation contains interbedded shale, siltstone, sandstone, and carbonaceous shale (Dubiel, 2000).

The Ferron Sandstone, a thin member of the Mancos Shale located stratigraphically below the Blackhawk Formation in Utah, is another coal-bearing unit utilized for underground mining in the Emery coal field (Macmillan et al., 1989). The mid-Turonian deltaic

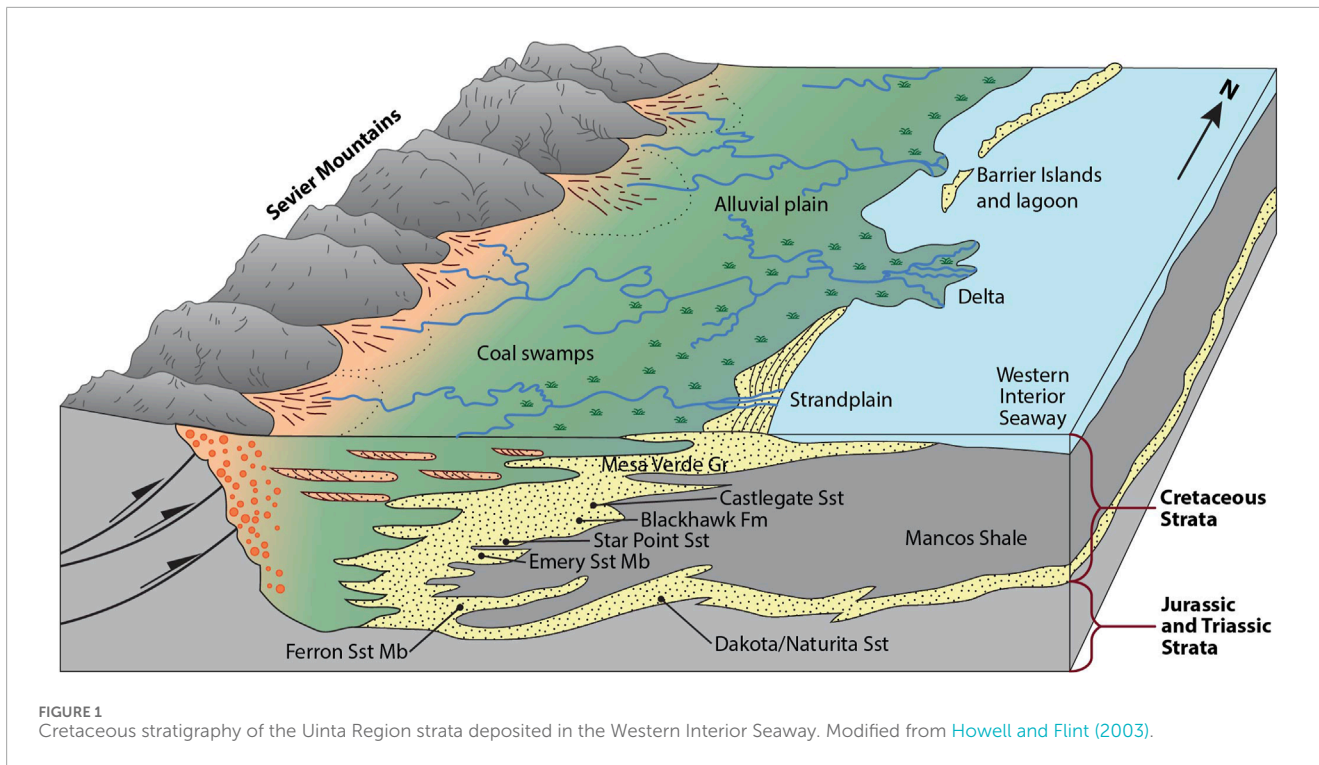


FIGURE 1 Cretaceous stratigraphy of the Uinta Region strata deposited in the Western Interior Seaway. Modified from Howell and Flint (2003).

sandstone unit consists of highly organized and well-documented lateral coal beds.

The Late Cretaceous, coal-bearing Mesaverde Group of western Colorado also records coastal plain to shallow marine deposition along the western margin of the Western Interior Seaway (Roehler et al., 1990; Stroker et al., 2013). Similar to the Blackhawk Formation, Mesaverde Group strata record clastic sediment transported eastward from the Sevier uplift and into the Western Interior Seaway (Madden et al., 1989; Roehler et al., 1990).

The upper portion of Colorado’s Mesaverde Group includes the Campanian Williams Fork Formation, which is the mining target of both Colorado mines included in this study (Roehler et al., 1990). This formation records the recession of the Western Interior Seaway with increasingly terrestrial strata overlying laterally extensive coastal plains and peat swamps (Stroker et al., 2013). Thick bituminous coal beds are found largely in the lower portion of the formation, as well as sandstone, shale, and carbonaceous shale deposits (Madden et al., 1989; Roehler et al., 1990).

The sedimentary strata observed in this region are generally composed of coal, siltstone, shale, and sandstone. Coal is defined as containing >50% terrestrial organic matter content by weight (Bustin, 1998; Neuendorf et al., 2011). The Cretaceous coals in the Blackhawk Formation, Ferron Sandstone, and Mesaverde Group are bituminous in rank. Shale and siltstone units frequently contain abundant terrestrial organic matter or carbonaceous material, but not enough to be defined as coal. Sandstone units typically contain less carbonaceous material than shales, siltstones, and coals, but may contain coal intraclasts and sedimentary structures typical of fluvial and coastal plain environments.

2.2 Study area and sampling

Samples for analysis were selected from six active mines, four historical/idle mines, four mine waste piles, and seven stratigraphically complete cores throughout the Uinta Region (Figure 2). There are currently four active coal mines in Utah, all underground operations in the Wasatch Plateau and Emery coal fields. These mines include Skyline mine in the northern Wasatch Plateau coal field, Gentry mine in the central Wasatch Plateau coal field, Emery mine in the Emery coal field, and Sufco mine in the southern Wasatch Plateau coal field (Table 1; Figure 2). Archived samples from the historical Star Point mine and Beaver Creek No. 8 mine in the Wasatch Plateau coal field, as well as the idled Dugout and Lila Canyon mines in the Book Cliffs coal field, were also included in this study (Table 1; Figure 2).

The analysis of Uinta Region coal also included samples from two operational underground mines in western Colorado: Deserado mine in the Lower White River coal field and West Elk mine in the Somerset coal field (Table 1; Figure 2). Material from four regional waste piles, two from active mines and two from historical mines, were also sampled and included in the dataset. The term “waste pile” is used broadly, with those at Star Point and Dugout being wash plant waste piles and those at Sufco and West Elk being mine waste piles. Within mine transects across the region, samples were collected across stratigraphic intervals depending on the feasibility of collection and access of resources. At Skyline mine, a vertical transect through the floor, coal seam, and roof of the Lower O’Connor B seam saw the collection of samples every 0.3–0.5 m (1–1.5 ft) throughout the 2.8 m (9.3 ft) transect. Similarly, at Skyline mine, samples were collected every 1–1.8 m (3–6 ft) across a 27.6 m (90.5 ft) horizontal transect through an igneous dike that crosscuts the Lower O’Connor B coal seam. Samples at Sufco mine were

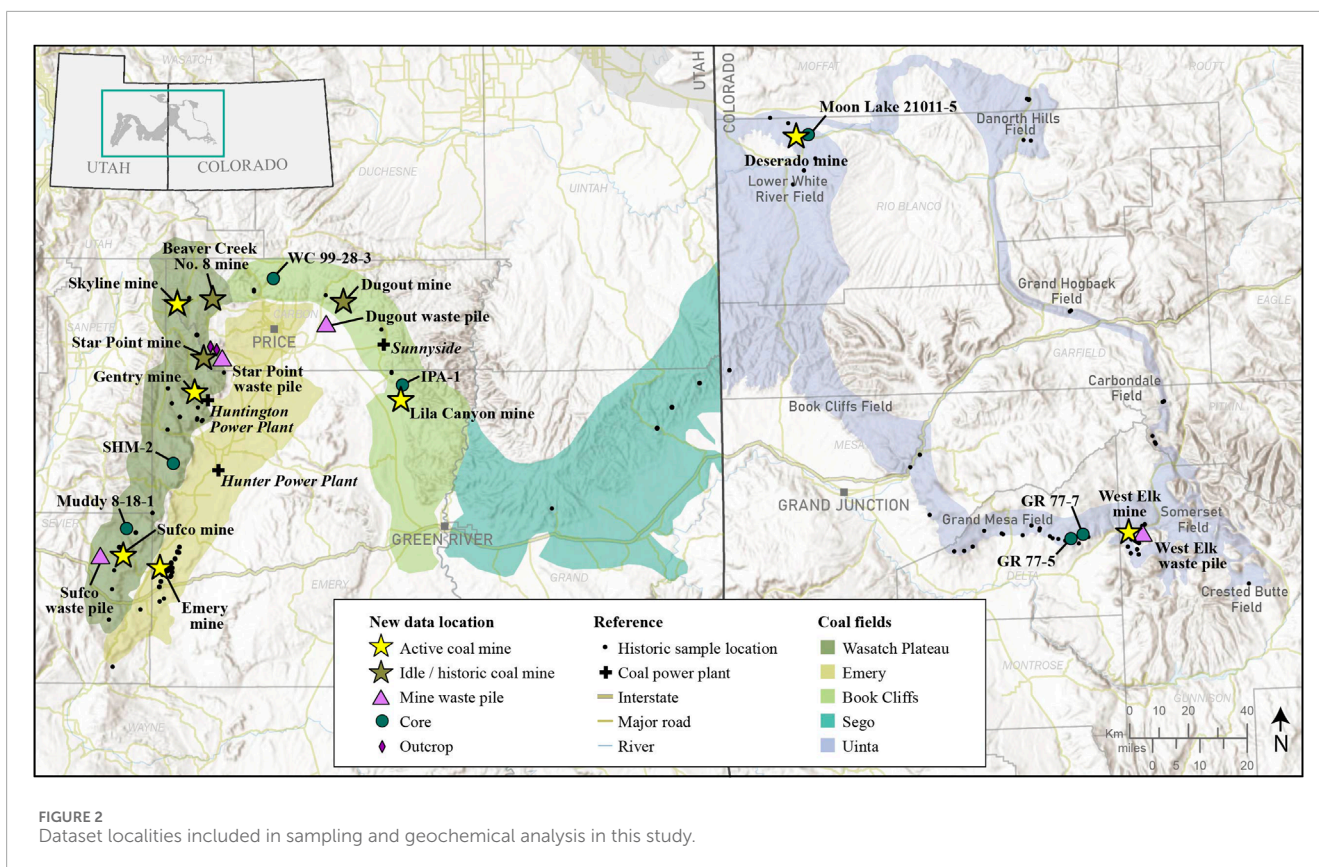


FIGURE 2 Dataset localities included in sampling and geochemical analysis in this study.

TABLE 1 Uinta Region mine and coal data.

Mine	Status	Coal field	Coal seam	Formation
Skyline	active	Wasatch Plateau	Lower O'Connor B	Blackhawk Formation
Gentry	active	Wasatch Plateau	Hiawatha and Blind	Blackhawk Formation
Sufco	active	Wasatch Plateau	Upper Hiawatha	Blackhawk Formation
Beaver Creek No. 8	historical	Wasatch Plateau	Castlegate A	Blackhawk Formation
Star Point	historical	Wasatch Plateau	Wattis	Blackhawk Formation
Lila Canyon	idle	Book Cliffs	Sunnyside	Blackhawk Formation
Dugout	idle	Book Cliffs	Rock Canyon and Gilson	Blackhawk Formation
Emery	active	Emery	I	Ferron Sandstone
Deserado	active	Lower White River	B	Mesaverde Group
West Elk	active	Somerset	E	Mesaverde Group

vertically sampled approximately every 0.6 m (2 ft) throughout a 17 m (55 ft) transect through the lower Hiawatha coal seam and various mudstone, siltstone, carbonaceous shale, and sandstone lithologies therein. At West Elk mine, samples were collected every 0.6 m (2 ft) along two 3 m (10 ft) vertical transects through the locally mined E seam. Additional E seam floor strata was collected at West Elk.

Historical mine samples were collected from the Utah Geological Survey archive, lacking stratigraphic context. Samples collected directly from waste piles, as well as run-of-mine samples, can be traced back to particular mines and mined seams.

Stratigraphically complete cores chosen for analysis include Utah's Muddy 8-18-1, SHM-2, WC 99-28-3, and IPA-1, and Colorado's Moon Lake 21011-5, GR 7-77-7, and GR-77-5 (Table 2;

TABLE 2 Uinta Region core and coal data.

Core	Depth (m)	Depth (ft)	Coal field	Coal seam	Formation
Muddy 8–18–1	121.9–335.3	400–1100	Wasatch Plateau	Hiawatha	Blackhawk Formation
SHM-2	320.0–341.4	1050–1120	Wasatch Plateau	Axel Anderson and Accord Lakes	Blackhawk Formation
WC 99–28–3	530.4–640.1	1740–2100	Book Cliffs	K2, K, C, A	Blackhawk Formation
IPA-1	457.2–518.2	1500–1700	Book Cliffs	Sunnyside	Blackhawk Formation
Moon Lake 21011–5	225.6–249.9	740–820	Lower White River	F, D, C-B, A	Mesaverde Group
GR-77–7	155.4–207.3	510–680	Grand Mesa	D, C, B, A	Mesaverde Group
GR-77–5	292.6–384.0	960–1260	Grand Mesa	E0, E1, D, C, B, A	Mesaverde Group

Figure 2). These cores were selected because, in most cases, 1) they cover the mined interval of interest, and 2) were located relatively close to active or recently active mine sites. Stratigraphically complete cores provide a valuable sampling opportunity, beyond the limited vertical sampling allowed in an active underground mine. Cores allow for further stratigraphic analysis, including coal-adjacent strata as well as coal seams.

The sampling of core was dependent upon the lithology of the stratigraphic section. Each sample was categorized into the following basic lithofacies scheme: 1) sandstone (coarse to fine-grained), 2) interlaminated sandstone and siltstone, 3) shale (commonly carbonaceous), 4) siltstone (commonly carbonaceous), 5) coal, and 6) igneous dikes. Sandstone units, which consistently recorded low REE enrichment in preliminary analyses, were sampled three times per unit—stratigraphic top, middle, and bottom. Interlaminated sandstone and siltstone, shale, siltstone, and coal units were sampled at 15 cm (0.5 ft) intervals. Additional high-resolution sampling at 3 cm (0.1 ft) intervals was conducted on REE-enriched 0.6–1.5 m (2–5 ft) thick siltstone and carbonaceous shale units found stratigraphically overlying or underlying coal seams.

2.3 Geochemical analysis

This study utilized an Olympus Vanta M series portable X-Ray Fluorescence (pXRF) as well as an 8900 Triple Quadrupole Inductively Coupled Plasma-Mass Spectrometry (ICP-MS) to quantify elemental abundances within samples. The typical approach to methodology throughout this study involved pXRF analysis of samples prior to ICP-MS analysis, due to the destructive sampling involved with ICP-MS. Despite the full-range-REE analysis provided by ICP-MS, pXRF offered a non-destructive, quick, and simple alternative method.

ICP-MS and pXRF are two analytical techniques with different principles, sensitivities, and capabilities, inherently leading to variations in their respective results. ICP-MS is a destructive method with low detection limits and a broad analytical range of REEs (Sc, Y, La, Ce, Pr, Nd, Sm, Eu, Gd, Tb, Dy, Ho, Er, Tm, Yb, Lu), while pXRF is a quick, non-destructive method with higher detection limits and a short analytical range of REEs (Sc, Y, La, Ce, Pr, Nd). Further, ICP-MS analyzes a larger volume of sample area compared

to pXRF. Due to these systematic differences, it is appropriate to predominantly employ pXRF for data analysis. The results between methods cannot be used interchangeably, but should instead be used complementary as illustrated in Figure 3 and Figure 4. Further evaluations of statistically significant variations between pXRF and ICP-MS datasets is in preparation, with preliminary results indicating statistically negligible differences via a proposed analytical methodology.

The pXRF analyzer was operated with Beam 1 at 40 kV for 45 s, Beam 2 at 10 kV for 30 s, and Beam 3 at 50 kV for 45 s. This study targeted the quantification of REEs detected via Beam 1 and 3, specifically including the following elements: Sc, Y, La, Ce, Pr, and Nd. Limits of detection are as follows: <25 ppm for Sc, <5 for Y ppm, and <10 ppm for La, Ce, Pr, and Nd. Notably, all pXRF analyses returned Sc values below the limit of detection, indicating low values of Sc within the targeted strata. These data agree with ICP-MS results, in which all samples recorded Sc values <25 ppm. Utilization of a 50 kV pXRF instrument is common and appropriate for quantifying REEs within sedimentary systems (Simandl et al., 2014a; Simandl et al., 2014b; Gallhofer and Lottermoser, 2018; Sterk et al., 2018; Gallhofer and Lottermoser, 2020). In total, 3,113 pXRF data points were collected.

Throughout pXRF analysis, a blank glass pellet and standard reference material (SRM), 2711a Montana II soil, were analyzed after every 20 analyses to verify instrument calibration. The SRM, standardized by the National Institute of Standards and Technology (NIST), includes 50 g of dried, powdered soil with moderately elevated trace element concentrations intended for use in the analysis of soils and sediment. Nine samples ranging in lithology also underwent repeated pXRF analysis without physical adjustment to guarantee precision. Repeated analyses of SRM show consistent instrument calibration throughout the project.

REE-enriched samples analyzed via pXRF were high-graded and selected for ICP-MS analysis at the University of Utah's ICP-MS Metals and Strontium Isotope Facility. The ICP-MS process combined incineration and acid digestion in a methodology suitable for the determination of trace elements in a range of sedimentary rocks. For each sample, ~40 g of rock was homogenized using a mortar and pestle to obtain 1) ~5 g of coarse 1 mm ground sample and 2) ~1 g of fine 0.1 mm ground sample. About 250 mg

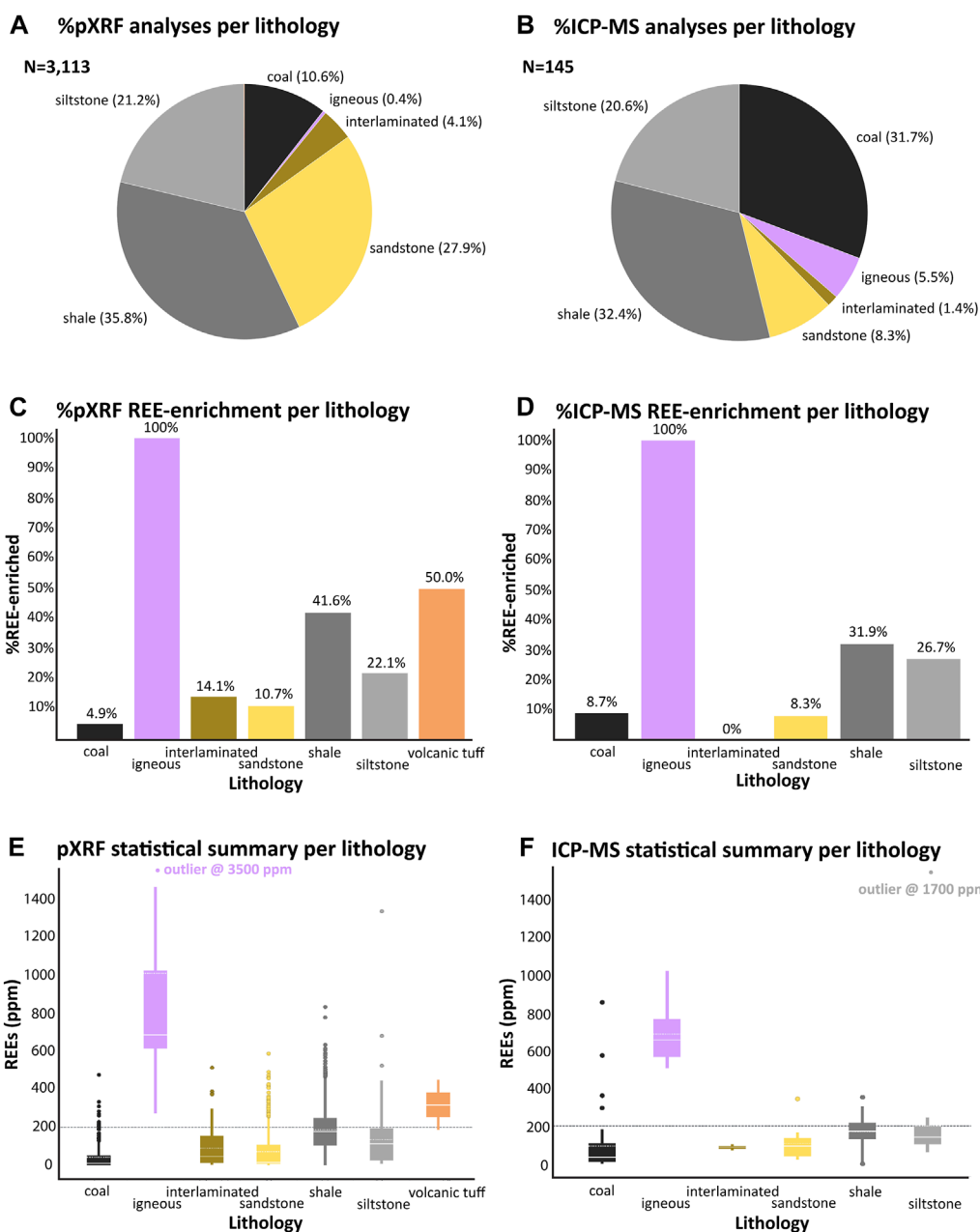


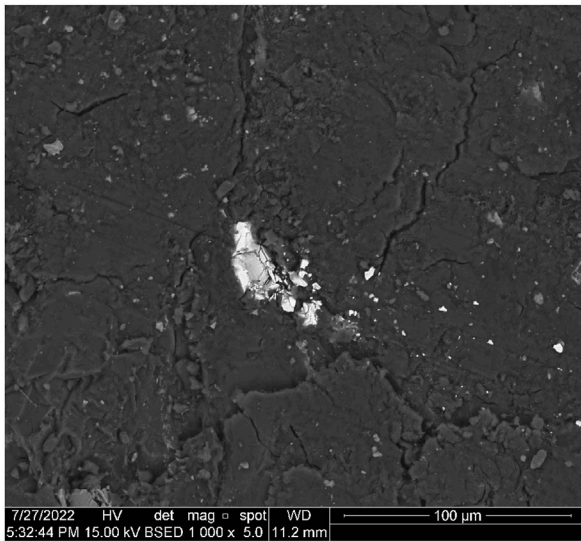
FIGURE 3 (A) Percentage of pXRF analyses performed on sample lithology; (B) Percentage of ICP-MS analyses performed on sample lithology; (C) Percentage of pXRF total analyses that show REE enrichment (>200 ppm), categorized by sample lithology; (D) Percentage of pXRF total analyses that show REE enrichment (>200 ppm), categorized by sample lithology; (E) box-and-whiskers plot of pXRF data presenting mean, median, quartile, and outlier data as compared to REE enrichment (200 ppm), categorized by sample lithology; (F) box-and-whiskers plot of ICP-MS data presenting mean, median, quartile, and outlier data as compared to REE enrichment (200 ppm), categorized by sample lithology.

of the fine-ground sample was incinerated in a lidded porcelain crucible at 550°C; the ashes were weighed, homogenized, and up to ~50 mg was transferred into a 7 mL polytetrafluoroethylene (PTFE) vial. Then, 2 mL of hydrofluoric acid (HF) and 1 mL of nitric acid (HNO₃)—both concentrated, trace metal grade quality—were slowly added. The vial was then closed and heated at 165°C for 3 days. The digest was then evaporated, and 2 mL of concentrated HCl was added. The vial was then closed and placed on a hot plate at 165°C for 2 days with occasional stirring. The

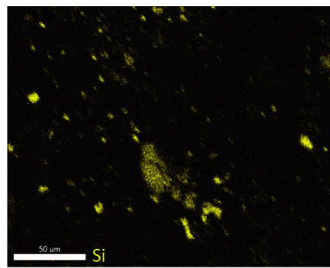
digests were then diluted by a factor of 100 using 2.4% HNO₃ and subsequently analyzed for REEs using a triple quadrupole inductively coupled plasma mass spectrometer (ICP-MS, Agilent 8900, Santa Clara, California). For details about quantification see the supplementary file. Data quality for both the digestion method and ICP-MS quantification was determined by using SRM SBC-1 (Brush Creek, PA shale), certified by the U.S. Geological Survey. A total of 145 data points was collected using the ICP-MS method.

Beaver Creek No. 8 mine, Castlegate A seam SEM-EDS

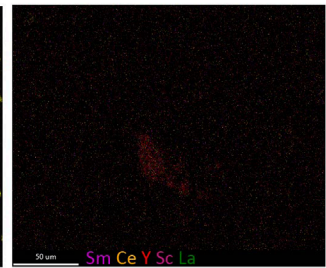
A Backscattered electron (BSE) image, 1000x



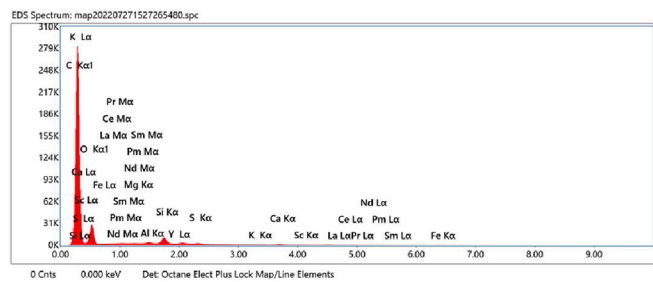
B EDS map Si



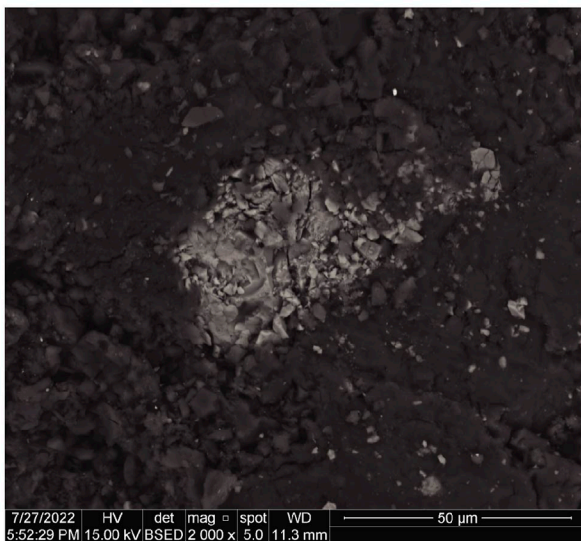
C EDS map REEs



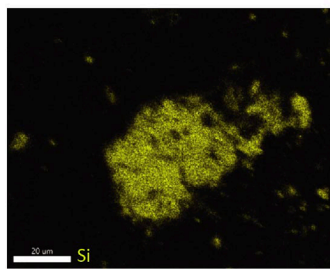
D EDS Spectrum



E Backscattered electron (BSE) image, 2000x



F EDS map Si



G EDS map REEs



H EDS Spectrum

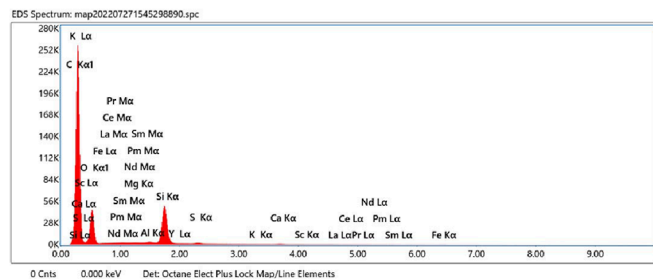


FIGURE 4

SEM-EDS imaging of REE enriched Beaver Creek mine coal sample; (A) Backscattered electron (BSE) image of silicate domains within sample, interpreted as a broken igneous crystal from volcanic debris; (B) EDS map of Si-rich igneous crystal domain; (C) EDS map showing REEs in Si-rich igneous crystal domain, including Sm, Ce, Y, Sc, La; (D) EDS Spectrum of sample (E) Backscattered electron (BSE) image of silicate domains within the sample; (F) EDS map of Si-rich igneous crystal domain; (G) EDS map showing REEs in Si-rich igneous crystal domain, including Sm, Ce, Y, Sc, La; (H) EDS Spectrum of sample.

Despite the consistent methodology of pXRF before ICP-MS analyses throughout this study, a subset of 31 samples collected for preliminary exploratory analysis in March 2022 from Gentry Mtn, Sufco, Emery, Lila Canyon, Dugout, Star Point, and Beaver Creek No.8 mines were analyzed first via ICP-MS. Then later, fine-grained powder split samples from the ICP-MS sample preparation process were packed into sediment pucks and analyzed via pXRF.

Two anomalously REE-enriched samples, a coal-adjacent carbonaceous shale sample from the Moon Lake 21011–5 core and an archived coal sample from the Beaver Creek No.8 Mine, were analyzed via Scanning Electron Microscopy/Energy Dispersive Spectroscopy (SEM-EDS) at the University of Utah's Biotechnology NanoFab Lab to image sample surfaces for elemental maps. SEM with EDS analysis utilized the FEI Quanta 600 FEG and EDAX

TABLE 3 Statistical summary by lithology.

Lithology	Analysis	N=	REE mean (ppm)	REE median (ppm)	% Samples REE enriched (>200 ppm)
coal	pXRF	329	42	10	4.9
	ICP-MS	46	94	35	8.1
shale	pXRF	1116	187	177	41.6
	ICP-MS	47	171	173	31.9
siltstone	pXRF	660	135	113	22.1
	ICP-MS	30	200	140	26.7
interlaminated	pXRF	128	90	46	14.1
	ICP-MS	2	88	88	0
sandstone	pXRF	868	71	15	10.7
	ICP-MS	12	107	95	8.3
igneous	pXRF	12	1005	681	100
	ICP-MS	8	689	657	100
volcanic tuff	pXRF	2	317	317	50.0

Octane elect SDD for this study. Samples were cut into pieces several centimeters in length using a rock saw and mounted on the SEM loading chamber such that a polished, flat surface on each sample was analyzed.

3 Results

Geochemical results include 3113 pXRF and 145 ICP-MS analyses of Uinta Region strata from six active coal mines, four historical/idle mines, four mine waste piles, and seven stratigraphically complete cores in geographic proximity to the active or recently active mines. The data include samples from a range of lithologies including coal, shale, siltstone, interlaminated sandstone and siltstone, sandstone, igneous dikes, and volcanic tuffs. The full data repository can be found at www.doi.org/10.7278/S50d-5ny1-1wc1.

The U.S. Department of Energy has established an REE enrichment cutoff of 300 ppm on a whole rock basis for concentrations to be considered economically viable (Bagdonas et al., 2022; Yesenchak et al., 2022; Kolker et al., 2024). In this study, REE concentrations greater than 200 ppm on a whole rock basis were considered REE enriched. This definition of enrichment is justified by the preliminary and exploratory nature of the study and the intention to maintain a liberal sample size without the elimination of potentially viable resources. Furthermore, because pXRF analyses only yield a subset of REE elemental data, it is logical to assume actual total REE concentrations in any one sample are higher than the pXRF analysis predicts.

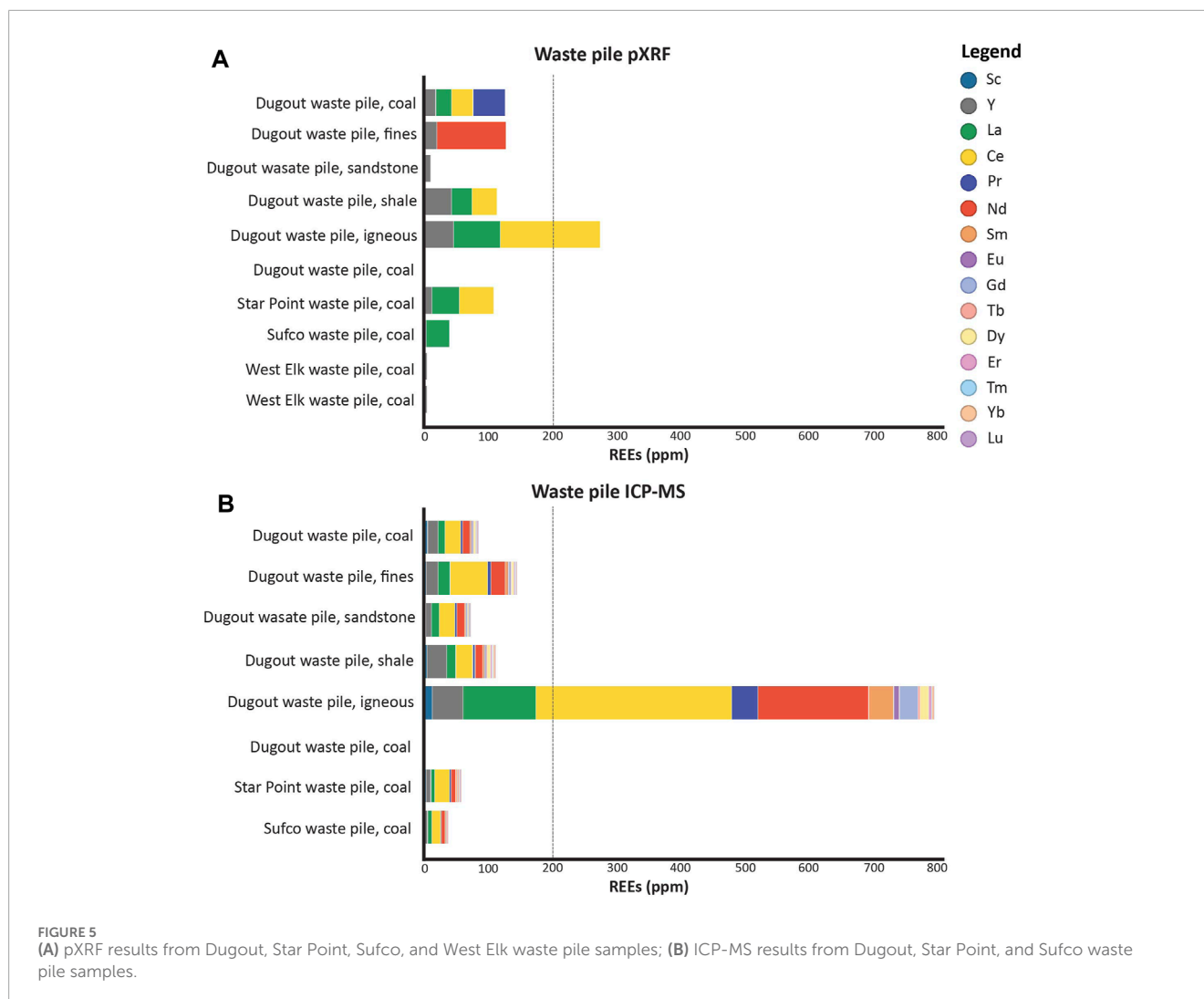
3.1 Lithologic trends

Shale and siltstone units, which are commonly carbonaceous, display the most promising REE enrichment within sedimentary systems analyzed in this study. Shale samples return REE enrichment values >200 ppm in 41.6% of pXRF analyses ($n = 1,116$) and 31.9% of ICP-MS values ($n = 47$) (Figure 3; Table 3). In contrast, siltstone samples display REE enrichment in 22.1% of pXRF analyses ($n = 660$) and 26.7% of ICP-MS analyses ($n = 30$) (Figure 3; Table 3).

Sandstone samples are less REE enriched, with 8.3% and 10.7% of samples displaying REE enrichment in both pXRF ($n = 868$) and ICP-MS ($n = 12$) analyses, respectively (Figure 3; Table 3). Similarly, 14.1% of interlaminated sandstone and siltstone samples show REE enrichment via pXRF ($n = 128$) and 0% via ICP-MS ($n = 2$) (Figure 3; Table 3).

A small population of coal samples, 4.7% of $n = 329$ pXRF analyses, show REE enrichment (Figure 3; Table 3). Coal samples that initially displayed REE enrichment via pXRF were high-graded for ICP-MS analysis, leading ICP-MS results to reflect a sampling bias. As such, all coal samples analyzed via ICP-MS reflect the highest pXRF-based enrichment throughout the sample area, resulting in a REE enrichment percentage of 8.7% ($n = 46$) as well as elevated mean and median values when compared to pXRF data (Figure 3; Table 3).

Despite generally low coal REE enrichment values, an archived Utah Geological Survey coal sample from the closed Beaver Creek No.8 Mine, Castlegate A seam, returned anomalously high REE enrichment values. ICP-MS-based total REE concentrations for these two analyses were 781 ppm and 934 ppm, respectively. Further



analyses via SEM-EDS at the University of Utah's NanoFab Lab revealed silicate domains interpreted as volcanic ash and debris transported via airfall (Figure 4), indicating that volcanic ash-rich coal could be a potential source for REEs.

All igneous samples (100%) analyzed via both pXRF and ICP-MS returned REE enrichment (Figure 3; Table 3). Samples from a 12 m (40 ft) igneous dike cross-cutting a coal seam at Skyline mine returned REE enrichment between 500 and 3500 ppm via pXRF analysis and 500 and 1000 ppm via ICP-MS. Samples of these local igneous dikes are also found in local waste piles, and contain similar REE enrichment to in-mine samples (Figure 5). Additional waste pile materials, including coal, sandstone, and shale lithologies, returned non-enriched REE results (<200 ppm) in both pXRF and ICP-MS analyses (Figure 5).

3.2 Stratigraphic trends

Results from pXRF and ICP-MS analyses support a general stratigraphic trend for the region, in which coal-adjacent beds composed of carbonaceous shale and siltstone commonly record

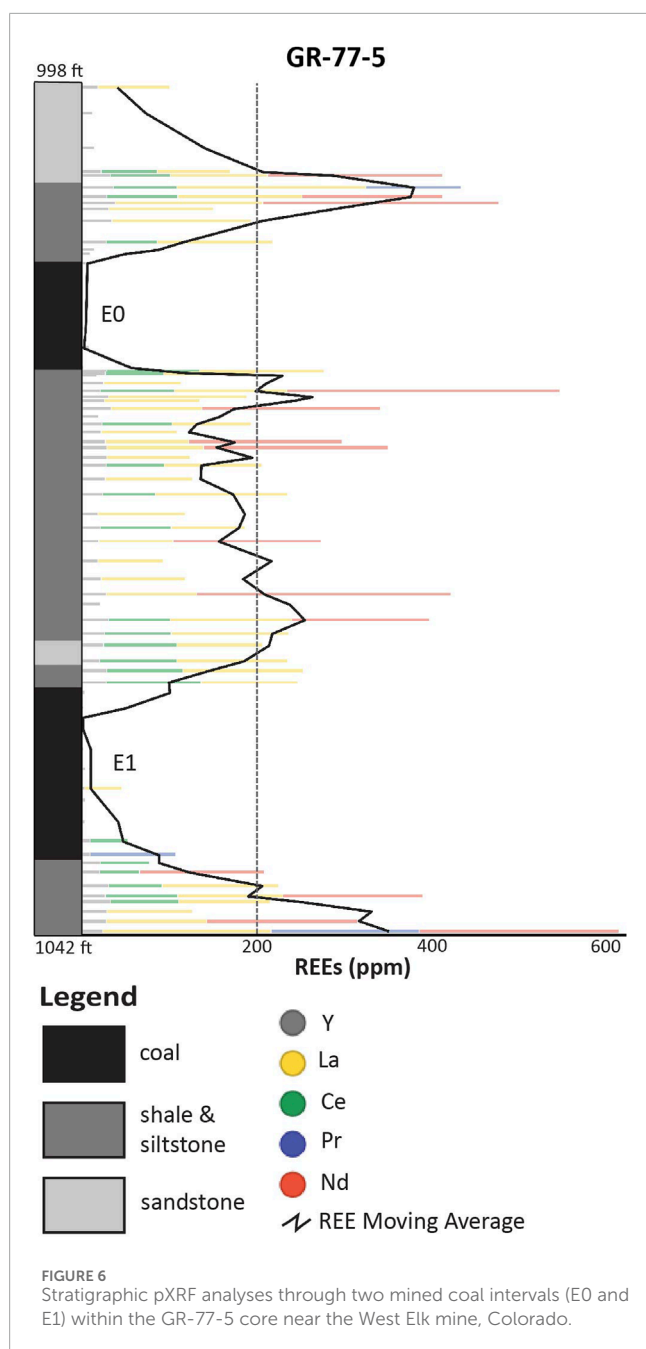
elevated values of REE concentrations (Table 4; Figure 6; Figure 7). Sandstone beds adjacent to coal seams less commonly record elevated REE concentrations. The coal seams themselves are also not commonly REE enriched.

Results suggest boundaries of enrichment above or below a specific coal seam are limited to within a 1.5 m (5 ft) margin, as detected in core data. Mean and median REE enrichment values within shale and siltstone beds are relatively greater within coal-adjacent boundaries in contrast to values representative of the whole core. Between 24% and 45% of coal-adjacent samples display REE enrichment via pXRF and ICP-MS analysis (Table 4). This specific stratigraphic pattern of REE enrichment in coal-adjacent carbonaceous siltstone and shale units is well documented in many of the core datasets and mine transects that were analyzed. Specifically, the GR-77-5 core located outside West Elk mine in Colorado documents REE enrichment within a 4.9 m (16 ft) shale and sandstone interval positioned stratigraphically between two actively mined coal beds (Figure 6).

Several notably enriched sections of coal-adjacent shale and siltstone underwent high-resolution pXRF analyses with 3 cm (0.1 ft) intervals where possible (Figure 7). These results indicate

TABLE 4 Statistical summary of coal-adjacent shale and siltstone.

Lithology	Analysis	N=	REE mean (ppm)	REE median (ppm)	% Samples REE enriched (>200 ppm)
shale	pXRF	685	194	184	44.7
	ICP-MS	34	169	176	29.4
siltstone	pXRF	320	148	123	23.8
	ICP-MS	20	143	129	25.0
combined	pXRF	1005	179	159	38.0
	ICP-MS	54	165	170	27.8



that REE enrichment is greatest within a 0.8 m (2.5 ft) coal-adjacent margin, with a “second peak” of enrichment observed between 0.9 m and 1.5 m (3 and 5 ft) from a coal bed. These 0.9–1.5 m (2–3 ft) thick margins of REE enrichment commonly contain significant individual values (>150 ppm) of the heavier elements detectable via pXRF, Pr and Nd. Other REEs (Y, La, Ce) commonly display consistent values throughout individual stratigraphic beds.

3.3 Geographic trends

The stratigraphic trends observed within this study can be placed within a geographic context, representing REE enrichment by coal field. REE enrichment is observed largely in carbonaceous siltstone and shale units adjacent to coal seams, but not all geographic locations return equally enriched carbonaceous shale and siltstone values (Table 5; Figure 8; Figure 9). For consistency, shale and siltstone samples have been binned, as have pXRF and ICP-MS results. Results indicate that the Uinta coal field strata of western Colorado present the most promising values of REE enrichment within coal-adjacent beds, specifically surrounding the West Elk mine (Table 5; Figure 8). Approximately 50.3% of coal-adjacent siltstone and shale within the Uinta coal field is REE enriched, compared to 24.4% from the Wasatch Plateau coal field of Utah and 27.7% from the Book Cliffs coal field of Utah (Table 5; Figure 9).

4 Discussion

4.1 Mechanisms of enrichment

The mechanisms of REE enrichment remain somewhat enigmatic, partly because enrichment across coal-bearing geographic regions has not yet been quantified within a geologic context. Stratigraphic trends identified in this study, however, suggest multiple variables control REE enrichment in both carbonaceous siltstone and shale, as well as coal units. Although it is not within the scope of this study to investigate the accurate processes of REE enrichment within these samples, various mechanisms have been documented within the literature with a range of relevance to this particular dataset. Possible controls on enrichment are outlined as follows.

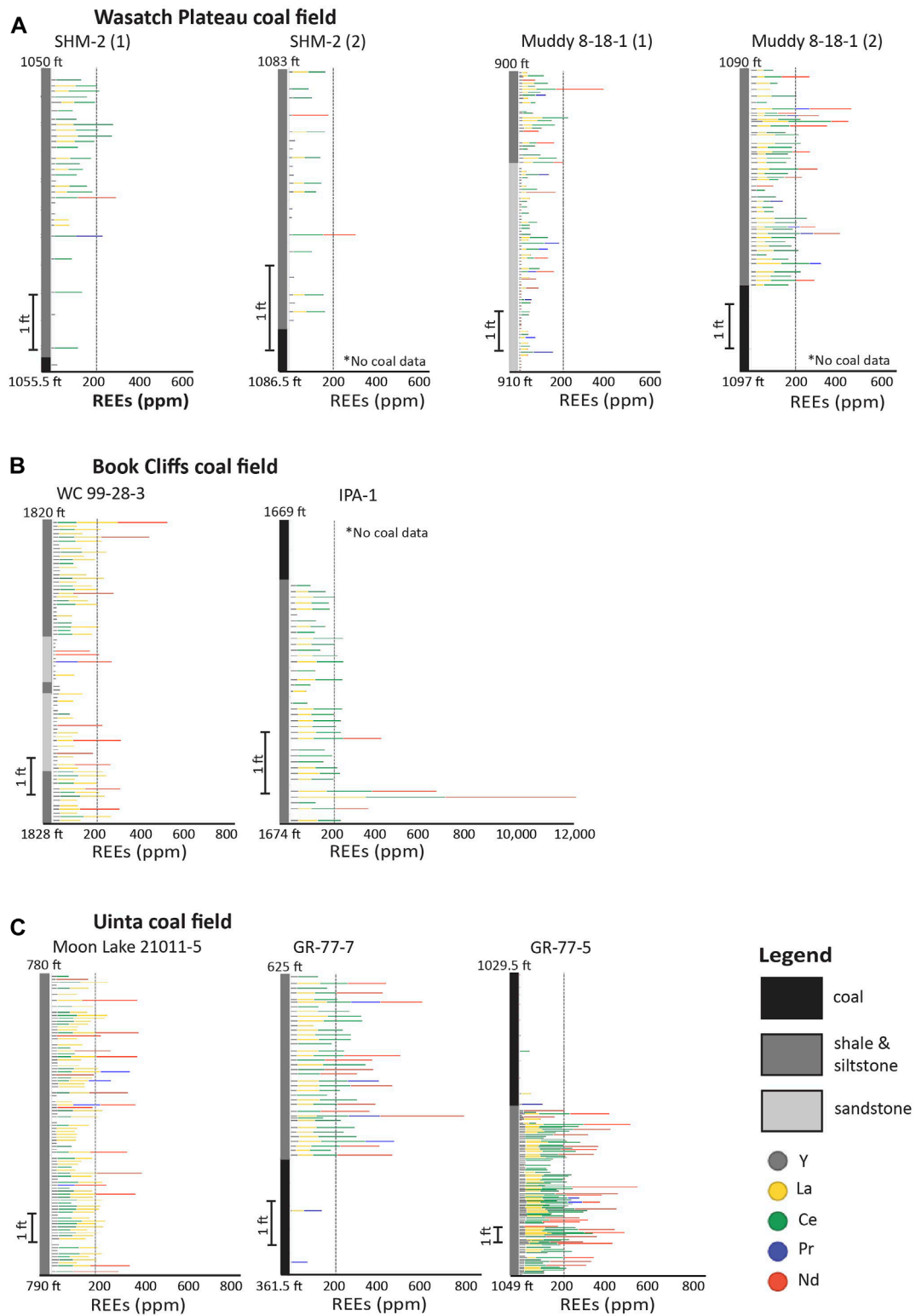


FIGURE 7 Stratigraphic high-resolution 3 cm (0.1 ft) pXRF analyses of coal, shale, siltstone, and sandstone beds in (A) the Wasatch Plateau coal field in Utah, (B) the Book Cliffs coal field in Utah, and (C) the Uinta coal field in Colorado.

TABLE 5 Statistical summary of coal-adjacent mudstone per coal field.

Coal field	N=	REE mean (ppm)	REE median (ppm)	% Samples REE enriched pXRF (>200 ppm)
Book Cliffs	267	159	135	27.7
Wasatch Plateau	291	138	130	24.4
Uinta	501	159	153	50.3

The factors controlling REE enrichment within coal deposits are dependent upon the geochemistry of the terrigenous source rocks and the influence of hydrothermal fluids, marine environments, percolating natural waters, volcanic ashes, and the overall sedimentary environment of the peat formation (Seredin and Dai, 2012; Dai et al., 2016). The distribution of REEs within organic and inorganic material directly relates to the depositional environment, and the strong correlation between REEs and humic substances can often be attributed to tuffaceous and hydrothermal mechanisms, coalification level, and interactions with ancient plants (Seredin and Dai, 2012; Chatterjee et al., 2022; Yesenchak et al., 2022; Creason et al., 2023; Hower et al., 2023).

A possible mechanism of enrichment pertaining to these samples involves a preliminary depositional and diagenetic multi-step model requiring the emplacement of REE source material within a host sediment.

REE-enriched mineral matter in coal can commonly be attributed to the deposition of volcanic ash during peat accumulation, with volcanic ash found in a variety of coal ranks from lignite to anthracite (Dai et al., 2017; Laudal et al., 2018; Dai et al., 2023). The presence of REE-enriched carbonaceous shale and siltstone sitting adjacent to coal can be attributed to volcanic ash fall within peat swamps and subsequent groundwater or hydrothermal enrichment. After REE-rich volcanic ash (i.e., tuffaceous material) settles into peat swamps, low-temperature water can leach REEs out of the humic material via early diagenetic processes (Seredin and Dai, 2012; Dai et al., 2017; Yesenchak et al., 2022; Creason et al., 2023). These elements can then be reabsorbed into overlying and underlying carbonaceous siltstone and shale beds. In this study, stratigraphic units of siltstone and shale within a 1.5 m (5 ft) coal-adjacent margin show up to 3.1% greater REE enrichment than the average values per lithology (Table 3; Table 4), supporting this claim. The Upper Cretaceous strata in the Uinta Region contain coal-adjacent, REE-rich carbonaceous shale and siltstone likely due to the abundance of volcanic ash fall during peat accumulation (Macmillan et al., 1989). SEM-EDS analysis reveals volcanic ash with ICP-MS-based REE enrichment of 781 ppm and 934 ppm, respectively, within coal from Utah's Beaver Creek No.8 Mine (Figure 4), supporting this hypothesis.

Igneous material reported in this study, specifically the 12 m (40 ft) dike recorded at Skyline mine, contains enriched values of REEs. There is much literary evidence of organic and inorganic alterations within coal-bearing sequences due to igneous intrusions (Fredericks et al., 1985; Snyman and Barclay, 1989; Ward et al., 1989; Rimmer et al., 2009; Yoksoulian et al., 2016; Sanders and Rimmer, 2020; Moura et al., 2021; Sanders et al., 2023). It has been shown

that contact metamorphism of igneous dikes into organic matter-rich coal can lead to devolatilization and ultimate REE-enrichment of the source rocks (Neumann et al., 2011; Moroeng et al., 2024). The coal samples surrounding igneous intrusions in this study do not speak to this mechanism, as samples do not record elevated REE concentrations (Figure 8). However, additional investigation into igneous intrusions within coal-bearing strata in the Uinta Region could offer more promising enrichment within surrounding coal.

There is also some consideration of the impact of diagenetic processes associated with coal rank (temperature, pressure, time) upon REE enrichment. Greater REE enrichment, specifically within heavy REEs (HREE), is seen in peats and low-rank coals due to the stronger HREE affinity for organic material (Eskenazy, 1999; Pédrot et al., 2010; Aide and Aide, 2012; Seredin and Dai, 2012; Eskenazy, 2015; Laudal et al., 2018; Bagdonas et al., 2022; Dai et al., 2023). This factor could also interact with the role of acidic waters and the preferential desorption of heavy REEs from clay-rich material (Eskenazy, 1999). This mechanism of enrichment is well documented in the literature with low-rank coal examples from North Dakota, Russia, and more (Laudal et al., 2018). As the collected data in this study exclusively pertain to bituminous coals, which share relatively similar burial diagenesis histories, the results from this study cannot be used to evaluate or isolate the impact of coal rank on the accumulation of REEs.

Alternatively, REE accumulation by plants can be considered a viable mode of enrichment, as a diverse group of ancient plant species is proposed to have been able to hyperaccumulate REEs with the interaction of hydrothermal fluids (Mohsin et al., 2019; Li et al., 2021; Mohsin et al., 2022; Hower et al., 2023b; Dai et al., 2023). This specific mechanism is well defined in bituminous coals sourced from Kentucky (Hower et al., 2023b). Considering the existence of peat swamps during the Cretaceous interval of deposition, REE enrichment via plant accumulation is a possible explanation, although these data do not speak directly to the proposed mechanism.

Further comparison of REE enrichment patterns across different coal regions is necessary to better understand and constrain the diagenetic and depositional mechanisms that control REE enrichment in coal-bearing strata. The total REE enrichment of an area is likely dependent upon multiple mechanisms, calling additional research to action.

4.2 Mining implications

This study suggests positive implications for mining operations, considering the stratigraphic trends observed in the results. REE

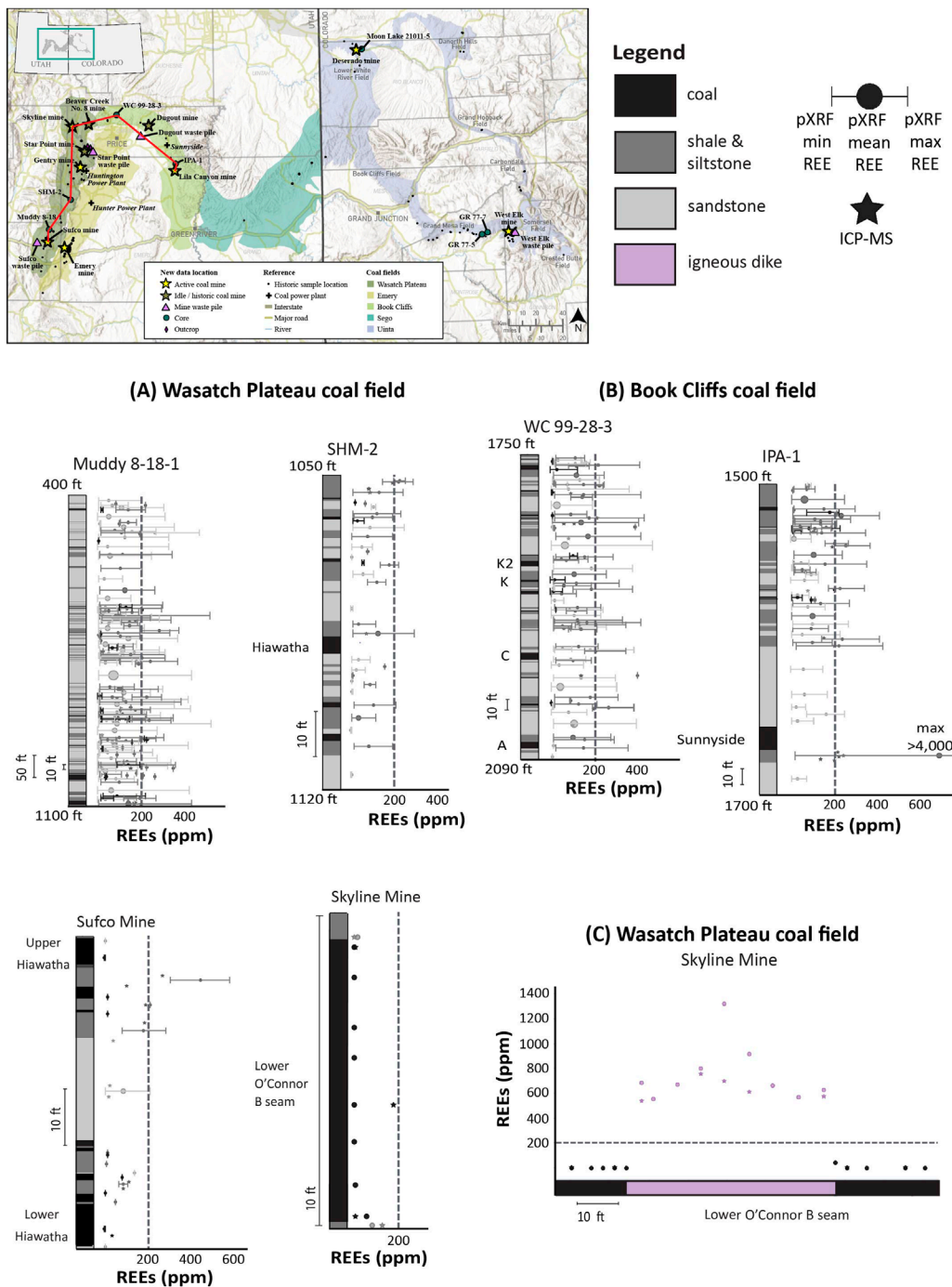
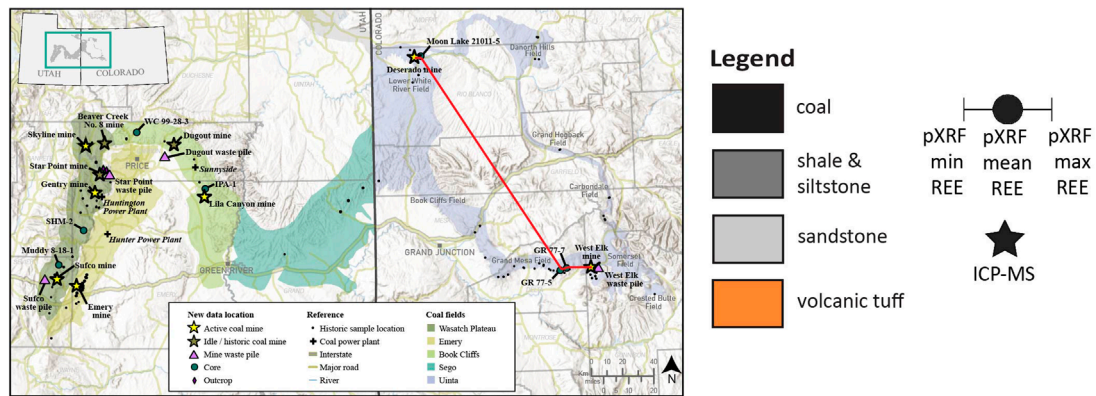


FIGURE 8 ICP-MS data points and pXRF data points per stratigraphic bed throughout core and mine transects within Utah's (A) Wasatch Plateau coal field, (B) Book Cliffs coal field, and (C) Wasatch Plateau coal field (Skyline Mine).

enrichment within coal-adjacent shale and siltstone encourages the mining potential of roof and floor strata relative to actively mined coal beds. As these coal-adjacent REE-enriched intervals are typically 0.6–5 m (2–5 ft) in thickness, there is great potential for active mines to expand their underground operations for the extraction and processing of shale and siltstone beds for REEs.

Igneous material can also be considered a promising, yet localized REE source within the Uinta Region. An *in-situ* igneous dike crosscutting an actively mined coal seam at the Skyline mine demonstrates REE enrichment >500 ppm over 12 m (40 ft) in width (Figure 8). This example is representative of igneous dikes throughout the local region and can encourage the economic viability of mining similar crosscutting dikes in coal seams.



Uinta coal field

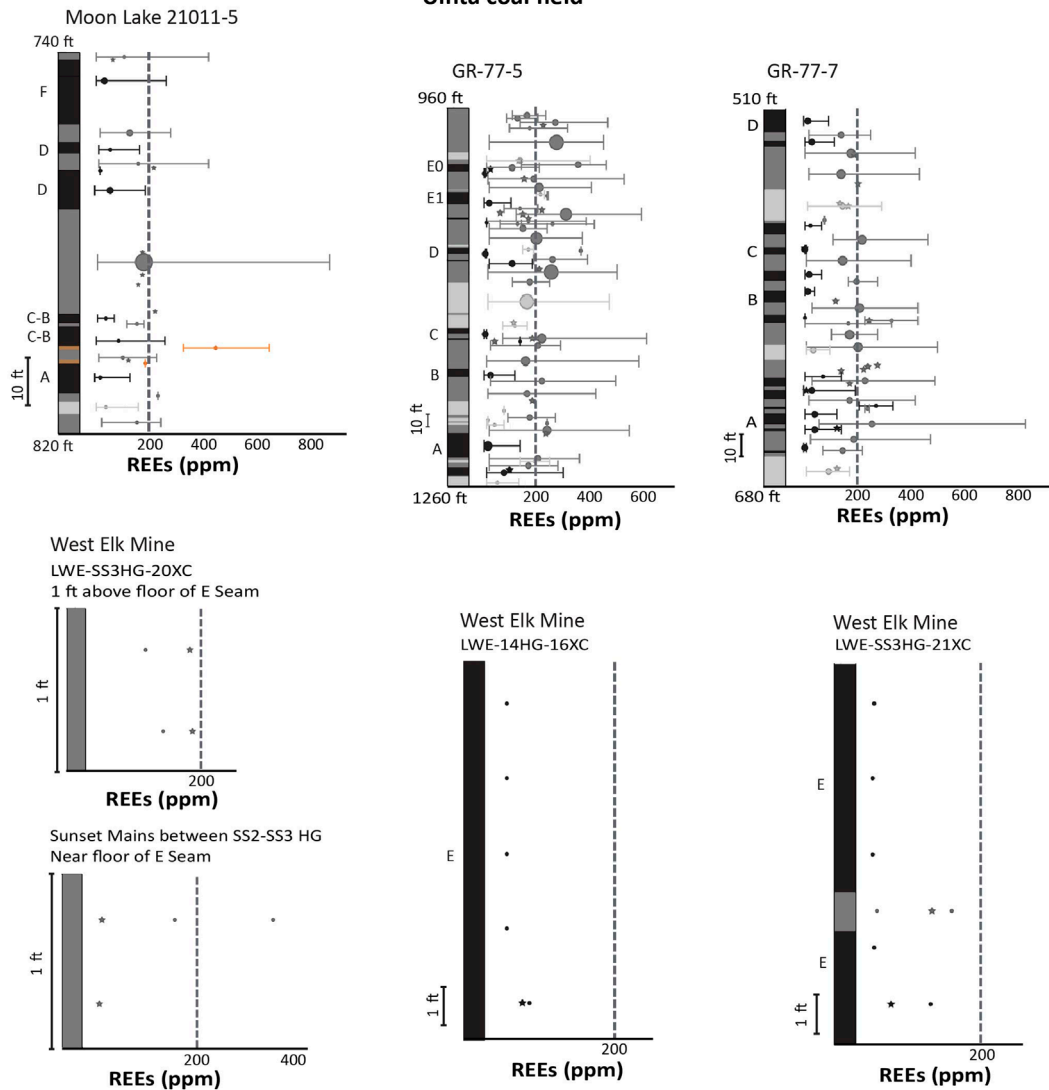


FIGURE 9 ICP-MS data points and pXRF data points per stratigraphic bed throughout core and mine transects within Colorado's Uinta coal field.

Further, igneous material and impure, volcanic-ash-rich coal are commonly discarded in regional coal mining waste piles. The extraction of these materials for REE processing could be economically and environmentally beneficial for active coal mines.

4.3 Conclusion

The results of this study suggest that carbonaceous shale and siltstone units directly stratigraphically above or below coal seams

within the Uinta Region show general trends of relative REE enrichment, with values >200 ppm. The enriched carbonaceous shale or siltstone units are typically 0.6–1.5 m (2–5 ft) in thickness above or below a coal seam, suggesting a diagenetic correlation between coal and carbonaceous shale or siltstone.

Greater REE enrichment (>500 ppm) is recorded within an igneous dike in an active mine that crosscuts a coal seam. The igneous dike is 12 m (40 ft) in width and is representative of common dikes in the local region. REE-enriched material from these igneous dikes typically end up in regional coal mining waste piles, inspiring their utilization for future REE processing.

Generally, pure coal samples lack REE enrichment. This study analyzed 329 Uinta Region coal samples via pXRF and 46 samples via ICP-MS, resulting in mean concentrations of 42 ppm and 94 ppm, respectively. Coals with high values of REEs, between 400 ppm and 900 ppm, are seen in a small population of coal samples rich with volcanic ash visible in SEM-EDS, suggesting a correlation between REE enrichment and igneous or volcanic components.

Data availability statement

The datasets presented in this study can be found in online repositories. The names of the repository/repositories and accession number(s) can be found in the article/Supplementary material.

Author contributions

HC: Conceptualization, formal analysis, investigation, methodology, visualization, Writing–original draft, Writing–review and editing. LB: Conceptualization, project administration, supervision, Writing–original draft, Writing–review and editing. DF: Methodology, Writing–original draft, Writing–review and editing. RG: Resources, visualization, Writing–review and editing. MV: Resources, Writing–review and editing. AG: Resources, Writing–review and editing.

References

- Aide, M. T., and Aide, C. (2012). Rare earth elements: their importance in understanding soil genesis. *ISRN Soil Sci.* 2012, 1–11. doi:10.5402/2012/783876
- Alonso, E., Sherman, A. M., Wallington, T. J., Everson, M. P., Field, F. R., Roth, R., et al. (2012). Evaluating rare earth element availability: a case with revolutionary demand from clean technologies. *Environ. Sci. Technol.* 46 (6), 3406–3414. doi:10.1021/es203518d
- Bagdonas, D. A., Enriquez, A. J., Coddington, K. A., Finnoff, D. C., McLaughlin, J. F., Bazilian, M. D., et al. (2022). Rare earth element resource evaluation of coal byproducts: a case study from the Powder River Basin, Wyoming. *Renew. Sustain. Energy Rev.* 158, 112148. doi:10.1016/j.rser.2022.112148
- Bustin, R. M. (1998). Coal: origin and diagenesis. *Geochemistry*, 90–92. doi:10.1007/1-4020-4496-8_58
- Chatterjee, S., Mastalerz, M., Drobniak, A., and Karacan, C. Ö. (2022). Machine learning and data augmentation approach for identification of rare earth element potential in Indiana Coals, USA. *Int. J. Coal Geol.* 259, 104054. doi:10.1016/j.coal.2022.104054
- Creason, C. G., Justman, D., Rose, K., Montross, S., Bean, A., Mark-Moser, M., et al. (2023). A geo-data science method for assessing unconventional rare-earth element resources in sedimentary systems. *Nat. Resour. Res.* 32, 855–878. doi:10.1007/s11053-023-10163-x
- Dai, S., Finkelman, R. B., Hower, J. C., French, D., Graham, I. T., and Zhao, L. (2023). *Inorganic geochemistry of coal*. Amsterdam: Elsevier, 438.
- Dai, S., Graham, I. T., and Ward, C. R. (2016). A review of anomalous rare earth elements and yttrium in coal. *Int. J. Coal Geol.* 159, 82–95. doi:10.1016/j.coal.2016.04.005
- Dai, S., Ward, C. R., Graham, I. T., French, D., Hower, J. C., Zhao, L., et al. (2017). Altered volcanic ashes in coal and coal-bearing sequences: a review of their nature and significance. *Earth-Science Rev.* 175, 44–74. doi:10.1016/j.earscirev.2017.10.005
- Dubieli, R. F. (2000). *Summary of geology and coal resources of the Blackhawk Formation in the southern Wasatch Plateau, central Utah geologic assessment of coal in the Colorado plateau*. Arizona, Colorado, New Mexico, and Utah: U.S. Geological Survey Professional Paper.
- Dushyantha, N., Batapola, N., Ilankoon, I. M. S. K., Rohitha, S., Premasiri, R., Abeyasinghe, B., et al. (2020). The story of rare earth elements (REEs): occurrences, global distribution, genesis, geology, mineralogy and global production. *Ore Geol. Rev.* 122, 103521. doi:10.1016/j.oregeorev.2020.103521

Funding

The author(s) declare that financial support was received for the research, authorship, and/or publication of this article. This work was supported by the U.S. Department of Energy's CORE-CM: Transforming Uinta Basin Earth Materials into Advanced Products project, DE-FE0032046.

Acknowledgments

Thank you to Skadi Kobe, Katie Cummings, and Tom Dempster at the Utah Geological Survey's Utah Core Research Center, as well as Amin Hamidat, Erin Starkie, Emma Morris, and Peyton Fausett from the University of Utah.

Conflict of interest

The authors declare that the research was conducted in the absence of any commercial or financial relationships that could be construed as a potential conflict of interest.

Publisher's note

All claims expressed in this article are solely those of the authors and do not necessarily represent those of their affiliated organizations, or those of the publisher, the editors and the reviewers. Any product that may be evaluated in this article, or claim that may be made by its manufacturer, is not guaranteed or endorsed by the publisher.

Supplementary material

The Supplementary Material for this article can be found online at: <https://www.frontiersin.org/articles/10.3389/feart.2024.1381152/full#supplementary-material>

- East, J. A. (2013). Coal fields of the conterminous United States—national coal resource assessment updated version: U.S. Geological Survey open-file report 2012–1205, one sheet. *scale 1*. doi:10.3133/ofr20121205
- Eskenazy, G. M. (1999). Aspects of the geochemistry of rare earth elements in coal: an experimental approach. *Int. J. Coal Geol.* 38 (3–4), 285–295. doi:10.1016/S0166-5162(98)00027-5
- Eskenazy, G. M. (2015). Sorption of trace elements on xylain: an experimental study. *Int. J. Coal Geol.* 150–151, 166–169. doi:10.1016/j.coal.2015.08.013
- Fredericks, P. M., Warbrooke, P., and Wilson, M. A. (1985). A study of the effect of igneous intrusions on the structure of an Australian high voltage bituminous coal. *Org. Geochem.* 8, 329–340. doi:10.1016/0146-6380(85)90012-9
- Gallhofer, D., and Lottermoser, B. G. (2018). The influence of spectral interferences on critical element determination with portable X-ray fluorescence (pXRF). *Minerals* 8, 320. doi:10.3390/MIN8080320
- Gallhofer, D., and Lottermoser, B. G. (2020). The application of pXRF for the chemical and mineralogical characterization of heavy mineral sands. *Geochem. Explor. Environ. Anal.* 20, 99–111. doi:10.1144/GEOCHEM2019-015
- Hampson, G. J. (2010). Sediment dispersal and quantitative stratigraphic architecture across an ancient shelf. *Sedimentology* 57 (1), 96–141. doi:10.1111/j.1365-3091.2009.01093.x
- Howell, J. A., and Flint, S. (2003). “Sedimentology and sequence stratigraphy of the Book Cliffs,” in *The Sedimentary record of sea-level change* (Ed G. Bearman) (The Open University), pp. 135.
- Hower, J. C., Eble, C. F., Dai, S., and Belkin, H. E. (2016). Distribution of rare earth elements in eastern Kentucky coals: indicators of multiple modes of enrichment? *Int. J. Coal Geol.* 160–161, 73–81. doi:10.1016/j.coal.2016.04.009
- Hower, J. C., Eble, C. F., Johnston, M. N., Ruppert, L. F., Hopps, S. D., and Morgan, T. D. (2023b). Geochemistry of the Leatherwood coal in eastern Kentucky with an emphasis on enrichment and modes of occurrence of rare earth elements. *Int. J. Coal Geol.* 280, 104387. doi:10.1016/j.coal.2023.104387
- Hower, J. C., Warwick, P., Scanlon, B. R., Reedy, R. C., and Childress, T. M. (2023a). Distribution of rare earth and other critical elements in lignites from the Eocene Jackson Group, Texas. *Int. J. Coal Geol.* 275, 104302. doi:10.1016/j.coal.2023.104302
- Humphries, M. (2011). Rare earth elements: the global supply chain. *Rare Earth Minerals Policies Issues*, 1–20.
- International Union of Pure and Applied Chemistry (IUPAC) (2005). *Nomenclature of inorganic chemistry, IUPAC recommendations 2005*. Cambridge, UK: RSC Publishing.
- Kauffman, E. G., and Caldwell, W. G. E. (1993). The western interior basin in space and time. *Geol. Assoc. Can. Special Pap.* 39 (July), 1–30.
- Kolker, A., Lefticariu, L., and Anderson, S. T. (2024). “Energy-Related rare earth element sources,” in *Rare earth metals and minerals industries* (Cham: Springer). doi:10.1007/978-3-031-31867-2_3
- Krahulec, K., and Bon, R. L. (2010). 2009 summary of mineral activity in Utah. *Utah Geol. Surv.* doi:10.34191/c-111
- Laudal, D. A., Benson, S. A., Palo, D., and Addleman, R. S. (2018). Rare earth elements in North Dakota lignite coal and lignite-related materials. *J. Energy Resour. Technol.* 140. doi:10.1115/1.4039738
- Leslie, H. F., Nordvig, M., and Brink, S. (2010). *Critical materials strategy 2010*. United States: U.S. Department of Interior, 1–166.
- Li, X., Xiao, J., Salam, M. M. A., Ma, C., and Chen, G. (2021). Impacts of bamboo biochar on the phytoremediation potential of *Salix psammophila* grown in multi-metals contaminated soil. *Int. J. Phytoremediation* 23, 387–399. doi:10.1080/15226514.2020.1816893
- Lin, R., Soong, Y., and Granite, E. J. (2018). Evaluation of trace elements in U.S. coals using the USGS COALQUAL database version 3.0. Part I: rare earth elements and yttrium (REY). *Int. J. Coal Geol.* 192, 1–13. doi:10.1016/j.coal.2018.04.004
- Liu, S., Nummedal, D., and Gurnis, M. (2014). Dynamic versus flexural controls of late cretaceous western interior basin, USA. *Earth Planet. Sci. Lett.* 389, 221–229. doi:10.1016/j.epsl.2014.01.006
- Long, K. R., Van Gosen, B. S., Foley, N. K., and Cordier, D. (2012). The principal rare earth elements deposits of the United States: a summary of domestic deposits and a global perspective. *Non-Renewable Resour. Issues Geoscientific Soc. Challenges*, 131–155. doi:10.1007/978-90-481-8679-2_7
- Macmillan, M. P., Crowley, S. S., Stanton, R. W., and Ryer, T. A. (1989). The effects of volcanic ash on the maceral and chemical composition of the C coal bed, Emery Coal Field, Utah. *Org. Geochem.* 14 (3), 315–331. doi:10.1016/0146-6380(89)90059-4
- Madden, D. J., Lujan, M., and Peck, D. L. (1989). *Stratigraphy, depositional environments, and paleogeography of coal-bearing strata in the upper cretaceous Mesaverde group, central grand hogback, garfield county, Colorado*. United States: US Geological Survey Professional Paper.
- Mancheri, N. A., Mancheri, N. A., Sprecher, B., Bailey, G., Ge, J., and Tukker, A. (2019). Effect of Chinese policies on rare earth supply chain resilience. *Resour. Conserv. Recycl.* 142, 101–112. doi:10.1016/j.resconrec.2018.11.017
- Mohsin, M., Kuittinen, S., Salam, M. M. A., Peräniemi, S., Laine, S., Pulkkinen, P., et al. (2019). Chelate-assisted phytoextraction: growth and ecophysiological responses by *Salix schwerinii* E.L Wolf grown in artificially polluted soils. *J. Geochem. Explor.* 205, 106335. doi:10.1016/J.GEXPLO.2019.106335
- Mohsin, M., Salam, M. M. A., Nawrot, N., Kaipainen, E., Lane, D. J., Wojciechowska, N., et al. (2022). Phytoextraction and recovery of rare earth elements using willow (*Salix* spp.). *Sci. Total Environ.* 809, 152209. doi:10.1016/j.scitotenv.2021.152209
- Moroeng, O. M., Murathi, B., and Wagner, N. J. (2024). Enrichment of rare earth elements in epigenetic dolomite occurring in contact metamorphosed Witbank coals (South Africa). *Int. J. Coal Geol.* 282, 104405. doi:10.1016/j.coal.2023.104405
- Moura, H., Moura, H., Suárez-Ruiz, I., Marques, M., Ribeiro, J., Ribeiro, J., et al. (2021). Influence of magmatic fluids on the organic and inorganic fractions of coals from the Peñarroya-Belmez-Espiel Basin (Spain). *Int. J. Coal Geol.* 235, 103679. doi:10.1016/J.COAL.2021.103679
- Neuendorf, K. K. E., Mehl, J. P., and Jackson, J. A. (2011). *Glossary of geology*. 5th ed. Alexandria, Virginia: American Geosciences Institute.
- Neumann, E.-R., Svensen, H., Galerne, C., Galerne, C., and Planke, S. (2011). Multistage evolution of dolerites in the karoo large igneous province, Central South Africa. *J. Petrology* 52, 959–984. doi:10.1093/PETROLOGY/EGR011
- Pédrot, M., Dia, A., and Davranche, M. (2010). Dynamic structure of humic substances: rare earth elements as a fingerprint. *J. Colloid Interface Sci.* 345 (2), 206–213. doi:10.1016/j.jcis.2010.01.069
- Rimmer, S. M., Yoksoulian, L. E., and Hower, J. C. (2009). Anatomy of an intruded coal, I: effect of contact metamorphism on whole-coal geochemistry, Springfield (No. 5) (Pennsylvanian) coal, Illinois Basin. *Int. J. Coal Geol.* 79, 74–82. doi:10.1016/J.COAL.2009.06.002
- Roberts, L. N. R., and Kirschbaum, M. A. (1995). *Paleogeography and the late cretaceous of the western interior of middle North America; coal distribution and sediment accumulation*. United States: US Geological Survey Professional Paper. doi:10.3133/pp1561
- Roehler, H. W., Lujan, M., and Peck, D. L. (1990). Stratigraphy of the Mesaverde group in the central and eastern greater green River Basin, Wyoming, Colorado, and Utah. *U. S. Geol. Surv. Prof. Pap.* doi:10.3133/pp1508
- Sanders, M. M., and Rimmer, S. M. (2020). Revisiting the thermally metamorphosed coals of the Transantarctic Mountains, Antarctica. *Int. J. Coal Geol.* 228, 103550. doi:10.1016/J.COAL.2020.103550
- Sanders, M. M., Rimmer, S. M., and Rowe, H. D. (2023). Carbon isotopic composition and organic petrography of thermally metamorphosed Antarctic coal: implications for evaluation of $\delta^{13}\text{C}_{\text{org}}$ excursions in paleo-atmospheric reconstruction. *Int. J. Coal Geol.* 267, 104182. doi:10.1016/j.coal.2022.104182
- Seredin, V. V., and Dai, S. (2012). Coal deposits as potential alternative sources for lanthanides and yttrium. *Int. J. Coal Geol.* 94, 67–93. doi:10.1016/J.COAL.2011.11.001
- Seredin, V. V., Dai, S., Sun, Y., and Chekryzhov, I. Y. (2013). Coal deposits as promising sources of rare metals for alternative power and energy-efficient technologies. *Appl. Geochem.* 31, 1–11. doi:10.1016/j.apgeochem.2013.01.009
- Simandl, G. J., Fajber, R., and Paradis, S. (2014b). Portable X-ray fluorescence in the assessment of rare earth element-enriched sedimentary phosphate deposits. *Geochem. Explor. Environ. Anal.* 14, 161–169. doi:10.1144/GEOCHEM2012-180
- Simandl, G. J., Stone, R. S., Paradis, S., Fajber, R., Reid, H. M., and Grattan, K. (2014a). An assessment of a handheld X-ray fluorescence instrument for use in exploration and development with an emphasis on REEs and related specialty metals. *Miner. Deposita* 49, 999–1012. doi:10.1007/S00126-013-0493-0
- Snyman, C. P., and Barclay, J. (1989). The coalification of South African coal. *Int. J. Coal Geol.* 13, 375–390. doi:10.1016/0166-5162(89)90100-6
- Sterk, R., Gazley, M. F., Gazley, M. F., Wood, M., Collins, K. S., and Collins, G. (2018). Maximising the value of Portable XRF data in exploration: an example from Marirongoe, Mozambique. *Geochem. Explor. Environ. Anal.* 18, 142–154. doi:10.1144/GEOCHEM2017-037
- Stroker, T. M., Harris, N. B., Crawford Elliott, W., and Marion Wampler, J. (2013). Diagenesis of a tight gas sand reservoir: upper cretaceous Mesaverde group, piceance basin, Colorado. *Mar. Petroleum Geol.* 40 (1), 48–68. doi:10.1016/j.marpetgeo.2012.08.003
- Taylor, K. G., Gawthorpe, R. L., and Fannon-Howell, S. (2004). Basin-Scale diagenetic alteration of shoreface sandstones in the upper cretaceous spring Canyon and aberdeen members, Blackhawk Formation, Book Cliffs, Utah. *Sediment. Geol.* 172 (1–2), 99–115. doi:10.1016/j.sedgeo.2004.08.001
- Ward, C. R., Warbrooke, P. R., and Roberts, F. I. (1989). Geochemical and mineralogical changes in a coal seam due to contact metamorphism, Sydney Basin, New South Wales, Australia. *Int. J. Coal Geol.* 11, 105–125. doi:10.1016/0166-5162(89)90001-3

- Weng, Z. H., Jowitt, S. M., Mudd, G. M., and Haque, N. (2014). Assessing rare earth element mineral deposit types and links to environmental impacts. *Trans. Institutions Min. Metallurgy, Sect. B Appl. Earth Sci.* 122 (2), 83–96. doi:10.1179/1743275813Y.0000000036
- Yesenchak, R., Sharma, S., and Maxwell, A. E. (2022). Modes of occurrence, elemental relationships, and economic viability of rare earth elements in West Virginia coals: a statistical approach. *Minerals* 12 (8), 1060. doi:10.3390/min12081060
- Yoksoulian, L. E., Rimmer, S. M., and Rowe, H. D. (2016). Anatomy of an intruded coal, II: effect of contact metamorphism on organic $\delta^{13}C$ and implications for the release of thermogenic methane, Springfield (No. 5) Coal, Illinois Basin. *Int. J. Coal Geol.* 158, 129–136. doi:10.1016/j.coal.2016.03.009
- Yoshida, S. (2000). Sequence and facies architecture of the upper Blackhawk Formation and the lower castlegate sandstone (upper cretaceous), Book Cliffs, Utah, USA. *Sediment. Geol.* 136, 239–276. doi:10.1016/S0037-0738(00)00104-4
- Young, R. G. (1955). Sedimentary facies and intertonguing in the upper cretaceous of the Book Cliffs, Utah-Colorado. *GSA Bull.* 66 (2), 177–202. doi:10.1130/0016-7606(1955)66[177:SFAHT]2.0.CO;2
- Zhang, L., Guo, Q., Zhang, J., Huang, Y., and Xiong, T. (2015). Did China's rare earth export policies work? - empirical evidence from USA and Japan. *Resour. Policy* 43, 82–90. doi:10.1016/j.resourpol.2014.11.007
- Zhou, B., Li, Z., and Chen, C. (2017). Global potential of rare earth resources and rare earth demand from clean technologies. *Minerals* 7 (11), 203. doi:10.3390/min7110203
- Zhou, B., Li, Z., Zhao, Y., Zhang, C., and Wei, Y. (2016). Rare Earth Elements supply vs. clean energy technologies: new problems to be solve. *Gospod. Surowcami Miner./Mineral. Resour. Manag.* 32 (4), 29–44. doi:10.1515/gospo-2016-0039